



This is a repository copy of *A Model-based Predictive Current Controller for a Back-to-Back Connected Multilevel Converter Aerospace Starter-Generator*.

White Rose Research Online URL for this paper:
<http://eprints.whiterose.ac.uk/104113/>

Version: Accepted Version

Proceedings Paper:

Williams, R., Foster, M.P. and Stone, D. (2016) A Model-based Predictive Current Controller for a Back-to-Back Connected Multilevel Converter Aerospace Starter-Generator. In: IECON 2016 - 42nd Annual Conference of the IEEE Industrial Electronics Society. IECON 2016 - 42nd Annual Conference of the IEEE Industrial Electronics Society, 24-27 Oct 2016, Florence, Italy. IEEE . ISBN 978-1-5090-3474-1

<https://doi.org/10.1109/IECON.2016.7793150>

© 2016 IEEE. Personal use of this material is permitted. Permission from IEEE must be obtained for all other users, including reprinting/ republishing this material for advertising or promotional purposes, creating new collective works for resale or redistribution to servers or lists, or reuse of any copyrighted components of this work in other works.

Reuse

Unless indicated otherwise, fulltext items are protected by copyright with all rights reserved. The copyright exception in section 29 of the Copyright, Designs and Patents Act 1988 allows the making of a single copy solely for the purpose of non-commercial research or private study within the limits of fair dealing. The publisher or other rights-holder may allow further reproduction and re-use of this version - refer to the White Rose Research Online record for this item. Where records identify the publisher as the copyright holder, users can verify any specific terms of use on the publisher's website.

Takedown

If you consider content in White Rose Research Online to be in breach of UK law, please notify us by emailing eprints@whiterose.ac.uk including the URL of the record and the reason for the withdrawal request.



eprints@whiterose.ac.uk
<https://eprints.whiterose.ac.uk/>

A Model-based Predictive Current Controller for a Back-to-Back Connected Multilevel Converter Aerospace Starter-Generator

R. H. Williams, M. P. Foster*, D. A. Stone
Department of Electronic and Electrical Engineering
The University of Sheffield
Sheffield, UK
*m.p.foster@sheffield.ac.uk

Abstract—The application of predictive current control to a multilevel converter is explored for application in an aerospace starter-generator system to investigate how such a system may be used to limit the harmonic distortion in the starter-generator's stator current waveform and also at the point of common connection with the aircraft supply system. The proposed system is analyzed, and a prototype converter and aerospace generator are used to provide experimental testing results. During testing a dynamometer is used to reproduce the turbines torque speed characteristics.

I. INTRODUCTION

The control of the power converter in aerospace Starter-Generator (S/G) systems is becoming a significant research area as engine manufacturers adopt this technology, within the More Electric Aircraft Initiative (MEAI) [1,2,3,7,9]. The power converter design for this application is challenging due to the operating requirements: the system must provide bi-directional power; have a wide operating speed range from standstill up to the S/Gs maximum speed; low weight and volume and comply with stringent aerospace standards [4,5]. Another desirable feature is the ability to minimize the harmonic content of the current waveforms at both the bus connection point and in the S/Gs stator [2,3]. Reducing stator current Total Harmonic Distortion (THD) permits the winding inductance to be used as the sole source of filtering therefore saving weight. Aerospace standards [4,5] impose stringent limits on the harmonic content of the current flowing at the distribution bus connection of power converters. Any method that enables power converters to reduce the THD at their bus connection is beneficial.

Improvement to a converter's power quality can be achieved through hardware modifications and control techniques. The simplest hardware modifications include increasing the switching frequency (f_s) or add additional choke inductance. Increasing f_s is not always feasible, particularly at increased high current ratings due to device limitations – ratings for S/G applications are typically 120 kVA or higher [6-9]. Although additional filtering may improve the power quality, it comes at the cost of increased system weight.

Converter topology has a great influence on power quality and there has been a lot of research into how multilevel

techniques may be used to reduce the THD whilst driving low inductance machines [2,3,10-13,19]. In [2,3] the application of a multilevel inverter to a S/G system was examined as a method to reduce THD. Improvements are also achievable through advanced modulation techniques and control and considerable research has been conducted on improving performance using predictive control techniques [14-19].

In this paper a Model-based Predictive Current Controller (MBPCC) is used to improve performance by using a model of the load and the power converter to predict the optimal switching states which will force the current towards the reference value [14-18]. In this study it is assumed that the electrical characteristics of both the power converter and S/G are known to reasonable accuracy and so compensation is not required to correct for model inaccuracies in this specific application. A description of the S/G system is provided along with an analysis of the multilevel topology adopted. The complete controller is discussed with emphasis placed on the mathematical models that form the backbone of the MBPCC. Experimental results are provided using the developed controller and a prototype converter. Experimental results, obtained using a conventional current controlled system, are also presented to allow comparisons to be drawn.

II. AEROSPACE STARTER-GENERATOR SYSTEMS

Aerospace gas turbines are typically started using an air driven starter turbine which is mechanically coupled to the compressor shaft. Compressed air is bled from the aircraft's Auxiliary Power Unit (APU) to supply the turbo starter [21,22]. A generator is also coupled to the engine shaft to supply the aircraft's electrical requirements. A key objective of the MEAI is the abandonment of pneumatic starters and separate generators in favour of an all-electric S/G thus reducing weight as the turbo-starter is no longer required.

The power converter is a key component in the S/G system. During starting mode the power converter draws electrical power from the APU and supplied to the S/G causing the turbine to accelerate. This process continues until the engine has reached the ignition speed (ω_i). At this point the engine may be ignited, thus it continues to accelerate under both its own power and that supplied by the S/G. Once the engine has reached idle speed

(ω_{idle}), it enters generating mode. The converter draws electrical power from the S/G to supply the aircraft's electrical loads which are connected to the distribution bus. Figure 1 provides a block diagram of the system showing the direction of electrical power flow in both modes of operation [2,3]. The torque-speed profile is described in further detail in Section V where the dynamometer emulator system is discussed.

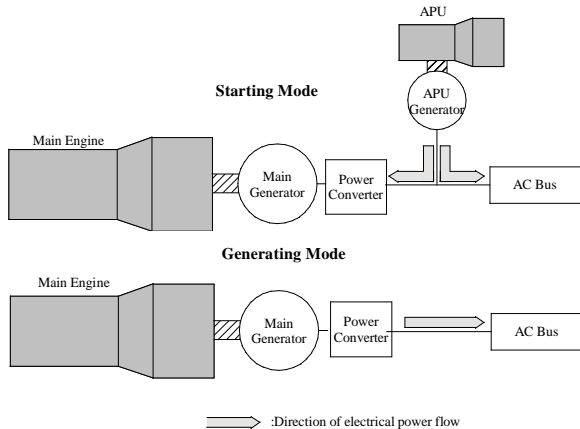


Fig. 1. Direction of power flow during both starting and generating modes

The majority of aerospace engines feature a Wound Field Synchronous Machine (WFSM) generator [3,7,20,22] since it provides easy regulation of the back-emf via the exciter winding. In [3] the authors undertook a study to determine what modifications were necessary to use a WFSM generator as a S/G and determined that it is necessary to adjust the excitation as a function of both the mode of operation and the generator speed as this maximizes the torque constant (K_T) during starting mode and regulates the back-emf as the machine speed varies during generating mode.

Future aircraft engines are likely to feature an embedded S/G to help to reduce mechanical complexity, save weight and improve serviceability [9]. To increase the power density of the S/G it is necessary to reduce the number of windings upon the stator [3] which also lowers the inductance. One of the aims of this work was to investigate how a multilevel inverter with MBPCC can be used to accommodate the reduced stator inductance while maintain good power quality.

III. MULTILEVEL CONVERTER DEVELOPMENT

There are numerous different multilevel converter topologies described in the literature. In [2,3,10,11,19,26,27] it is documented how the diode clamped configuration is particularly appropriate for drive applications. This topology when constructed in a back-to-back configuration supports bidirectional power flow which is essential in S/G systems. The reduction in THD in the current waveform is apparent in both the machine stator and at the point of coupling to the distribution bus. The back-to-back connected diode clamped inverter also has the advantage of not requiring any isolated DC sources. This gives the topology a significant advantage over the commonly used cascaded-H-bridge inverter where the provision for isolated DC sources would require a multiple winding transformer with separate rectifiers for each source and this would add significant weight and complexity.

A five level diode-clamped configuration is used throughout this study since it offers greater reduction in THD than the more common three-level, Neutral-Point-Clamped (NPC) inverter. The schematic for the five-level, back-to-back connected, diode clamped converter used throughout this study is shown in Figure 2. The convention used throughout this paper is that Unit 1 and Unit 2 refer to the bus connected and machine connected inverters respectively. The units are connected together via a four level DC link containing a capacitor bank to provide decoupling [10].

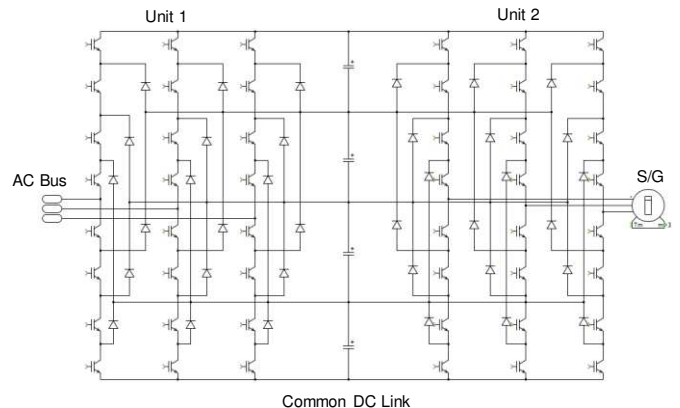


Fig. 2. Five-level back-to-back connected diode-clamped multilevel converter

IV. CONVERTER CONTROL SYSTEM

A. Conventional Field Oriented Controller

It is the norm in power electronics when dealing with three phase converters to utilize Field Orientated Control (FOC) to simplify control operations [24-26]. Three phase variables ($x_{a,b,c}$) are transformed into two orthogonal vectors ($x_{d,q}$) on a synchronously rotating reference frame (d & q) using (1). Here θ represents the electrical angular displacement which is equal to the rotor angle multiplied by the number of pole pairs (p). This greatly simplifies the control structure greatly as the three-phase signals are transformed into two DC signals allowing simple Proportional-Integral (PI) controllers to be used [25,26]. In the case of a synchronous machine drive, the convention states that the d axis is aligned with the rotor's flux. For the reasons outlined above, the stator current (I) is transformed using (1) yielding I_d and I_q . In the case of a synchronous machine drive, the torque produced by the motor is proportional to I_q .

$$\begin{bmatrix} x_d \\ x_q \end{bmatrix} = \begin{bmatrix} \cos(\theta) & \cos(\theta - 2\pi/3) & \cos(\theta + 2\pi/3) \\ -\sin(\theta) & -\sin(\theta - 2\pi/3) & -\sin(\theta + 2\pi/3) \end{bmatrix} \begin{bmatrix} x_a \\ x_b \\ x_c \end{bmatrix} \quad (1)$$

During starting mode, Unit 2 is tasked with accelerating the engine up to ω_{idle} and so a secondary PI control loop is used as a speed regulator, generating an I_q demand value (I_q^*). The d component (I_d) does not contribute to the torque and is therefore minimized ($I_d^*=0$) [2,3,10]. Two PI regulators are then used to determine the converter output voltages V_d and V_q necessary to make $I_q=I_q^*$ and $I_d=I_d^*$. A Space Vector Modulator (SVM) is used to select the appropriate switching combination to produce V_d and V_q at the converter output. The same SVM is used in both the conventional controller and also the MBPCC. A block diagram of the controller is shown in Figure 3.

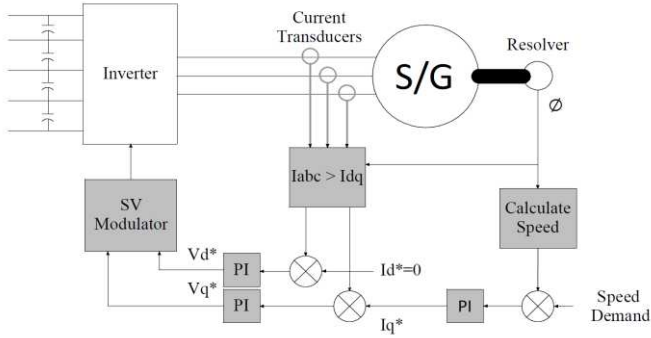


Fig. 3. Field oriented controller for Unit 2

During generating mode the controller for Unit 2 is modified to ensure that the DC link voltage is always maintained at the required amplitude (V_{DC}^*). A PI loop is employed, which compares V_{DC} to V_{DC}^* , in order to produce I_q^* . A more extensive description of the FOC used in this study may be found in [2] and [3].

The SVM translates V_d & V_q into appropriate switching states for the 3-phase inverter. The demand values to be synthesized are first transformed into two orthogonal vectors (α and β) on a stationary reference frame using the inverse of Park's transformation (2) [24-26].

$$\begin{bmatrix} V_\alpha \\ V_\beta \end{bmatrix} = \begin{bmatrix} \cos(\theta) & -\sin(\theta) \\ \sin(\theta) & \cos(\theta) \end{bmatrix} \begin{bmatrix} V_d \\ V_q \end{bmatrix} \quad (2)$$

The projection of V_α and V_β onto the SV diagram may then be calculated. This is a vector of length V_{ref} , and with an angular displacement from the α axis of ϕ . This can then be visualized onto a SV diagram (Figure 4) where the various switching vectors of the converter are displayed. For clarity only the switching vectors located on the perimeter of the hexagon are labeled. The vector "420" details the switch configuration of phases A, B and C respectively where the number dictates the output phase voltage should that vector be selected. Convention here is 4, 3, 2, 1 and 0 represent phase voltages V_{dc} , $3V_{dc}/4$, $V_{dc}/2$, $V_{dc}/4$ and 0V respectively. It is the task of the SVM to determine the nearest three vectors to V_{ref} for each switching cycle. By applying these vectors for calculated duty cycles, V_{ref} is synthesized at the converter output. A more comprehensive description of SVM including all relevant equations is provided in [24].

The SVM is also responsible for the balancing of the capacitor voltages [10,13,26] of the multilevel converter system ensuring that the voltage of each capacitor (V_{cx}) is equal (i.e. $V_{cx}=V_{dc}/4$). With the exception of the vectors located on the SV diagram perimeter, multiple vectors occupy the vertices of each triangle shown in Figure 4. Reference [26] described a technique for achieving voltage balancing through careful selection of the redundant vectors. A similar technique was used in this study.

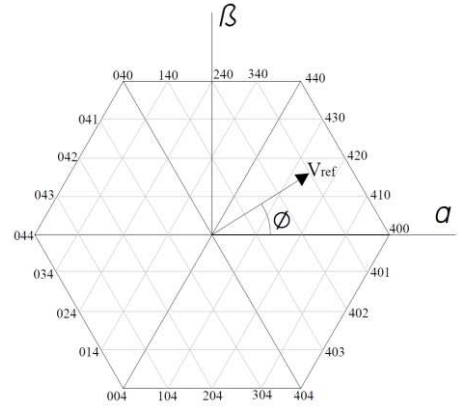


Fig. 4. Space vector diagram for five level, diode clamped multilevel converter

B. Proposed model-based predictive current controller

In conventional FOC PI controllers are used to drive the stator current errors to zero. The proposed MBPCC is different in that a model of the machine/load is employed to generate the values of V_d and V_q necessary to produce the required stator current. The values of V_d and V_q are then passed to the SVM.

The three phase equations for a synchronous machine are given in (3). Here R_s , L_s , ω_m , θ_e and λ_m represent stator winding resistance, synchronous inductance, machine angular velocity, electrical angle and machine flux linkage respectively.

$$\begin{bmatrix} V_a \\ V_b \\ V_c \end{bmatrix} = \begin{bmatrix} R_s & 0 & 0 \\ 0 & R_s & 0 \\ 0 & 0 & R_s \end{bmatrix} \begin{bmatrix} I_a \\ I_b \\ I_c \end{bmatrix} + \begin{bmatrix} L_s & 0 & 0 \\ 0 & L_s & 0 \\ 0 & 0 & L_s \end{bmatrix} \frac{d}{dt} \begin{bmatrix} I_a \\ I_b \\ I_c \end{bmatrix} - \omega_m \lambda_m \begin{bmatrix} \sin(\theta_e) \\ \sin(\theta_e - 2\pi/3) \\ \sin(\theta_e - 4\pi/3) \end{bmatrix} \quad (3)$$

Equation (3) may be transformed into the d-q domain using (1) to yield (4). L_d and L_q represent the d and q components of the synchronous inductance. K_e is the back-emf constant of the machine and ω_e the electrical angular velocity.

$$\begin{bmatrix} V_d \\ V_q \end{bmatrix} = \begin{bmatrix} R_s & -\omega_e L_q \\ \omega_e L_d & R_s \end{bmatrix} \begin{bmatrix} I_d \\ I_q \end{bmatrix} + \begin{bmatrix} L_d & 0 \\ 0 & L_q \end{bmatrix} \frac{d}{dt} \begin{bmatrix} I_d \\ I_q \end{bmatrix} + \begin{bmatrix} 0 \\ K_e \omega_m \end{bmatrix} \quad (4)$$

So that (4) may be efficiently implemented within the digital signal processor (DSP) it is first transformed into a discrete-time form (6) and (7) [15,16]. To do this the derivative in (4) is approximated using (5) [15], where T_s is the sampling period and k is the present time sample.

$$\frac{dI}{dt} \approx \frac{I[k] - I[k-1]}{T_s} \quad (5)$$

$$V_q[k] = R_s I_q[k] + \frac{L_q}{T_s} (I_q[k+1] - I_q[k]) + L_d \omega_e[k] I_d[k] + K_e \omega_m[k] \quad (6)$$

$$V_d[k] = R_s I_d[k] + \frac{L_d}{T_s} (I_d[k+1] - I_d[k]) - L_q \omega_e[k] I_q[k] \quad (7)$$

Equation (6) and (7) can be modified for use in a MBPCC by shifting the equation one discrete time step forward [15], and substituting $I[k+1]$ for $I^*[k+1]$. The equations now calculate the necessary converter output voltage (V_d and V_q) to apply next

time step $[k+1]$, in order to force the current in the next time step $I[k+1]$ to the demand value $I^*[k+1]$.

The outer control loop that generates $I^*[k+1]$ is of sufficiently lower bandwidth than the current controller that it can be safely assumed that $I^*[k+1] = I^*[k]$. It is also assumed that the rate of change of the S/G speed is low, so that the substitution $\omega_m[k+1] \approx \omega_m[k]$ is valid providing the MBPCC.

$$V_q[k+1] = R_s I_q^*[k] + \frac{L_q}{T_s} (I_q^*[k] - I_q[k]) + L_d \omega_e[k] I_d^*[k] + K_e \omega_m[k] \quad (8)$$

$$V_d[k+1] = R_s I_d^*[k] + \frac{L_d}{T_s} (I_d^*[k] - I_d[k]) - L_q \omega_e[k] I_q^*[k] \quad (9)$$

Voltages V_d and V_q can now be converted into the $(\alpha \beta)$ domain using (2) and implemented by the SVM described earlier in the next time step.

V. EXPERIMENTAL SET UP

A. Prototype Converter

A 10kW five-level, diode clamped, back-to-back connected converter (Figure 5) was used for evaluating the controller. Each Unit has a dedicated DSP based controller coupled to a Field Programmable Gate Array (FPGA) which generated the gate signals for the IGBTs.

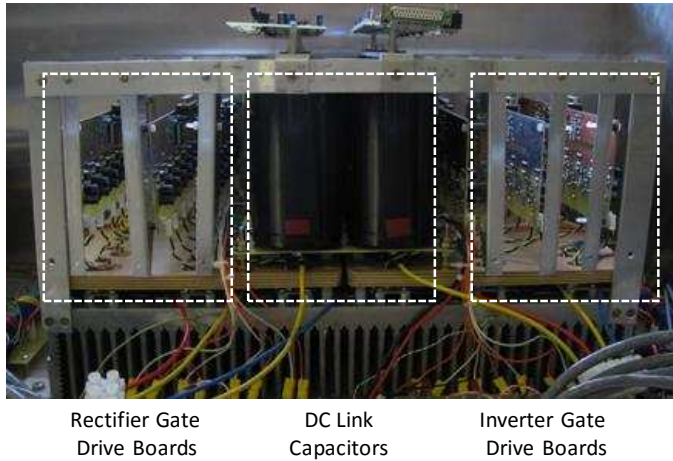


Fig. 5. Prototype converter system

B. Load Machine and Dynamometer Set Up

A 50kW WFSM removed from a Rolls Royce Artouste engine is used as the S/G. The parameters for this machine are given in Table II.

Since it was unfeasible to perform S/G testing whilst the machine is still mounted to the engine due to the cost and danger of igniting the turbine a dynamometer was used to emulate the torque-speed profile of the turbine. Similar to [2,3] a LabView based program monitors both the speed of the S/G and also the mode of operation, the required torque and speed are then calculated and sent to a Control Techniques drive, which was connected to the dynamometer. A block diagram of this setup is shown in Figure 6.

TABLE II

Parameter	Value
Rated Power	50 kW
Rated Speed	6000 rpm
Pole Pairs	4
Stator Synchronous Inductance	36 μ H
Stator Resistance	300m Ω
Exciter Winding Inductance	12mH
Exciter Winding Resistance	3.3 Ω

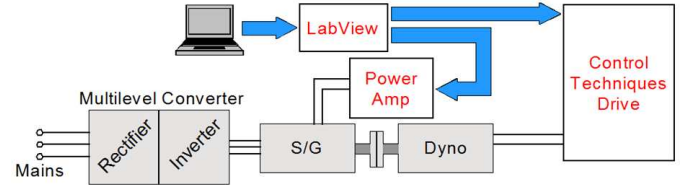


Fig. 6. Block diagram of LabView controlled test system

The torque produced by the dynamometer is dependent on the mode of operation. The complete torque-speed profile is shown in Figure 7. During starting mode the turbine is initially modeled as a fan load with some additional friction between standstill and ω_i . Upon reaching ω_i it is assumed that the engine is ignited and begins to produce some torque to supplement that provided by the S/G. This behavior is apparent in Figure 7, as the loading torque linearly reduces as the S/G accelerates. This process continues until a velocity of ω_{idle} has been achieved and now the dynamometer torque has become positive. At this point it is assumed that the turbine has reached its self-sustaining speed and therefore no longer requires the torque input from the S/G to maintain rotation. It is at this point that the S/G and power converter make the transition between starting and generating mode. Power flow is therefore reversed. The dynamometer accelerates up to the engines maximum operation speed ω_c . This signifies an engine being throttled for takeoff after being started. The dynamometer maintains a constant velocity of ω_c after this process has finished, regardless of the loading placed upon it by the S/G. This is to be expected as the mechanical loading placed upon an engine due to the generator is small in comparison to the loading placed upon an engine due to thrust production. A generator would therefore have minimal effect of the rotation speed of the engine.

During testing ω_i , ω_{idle} and ω_c were set to 700 rpm, 1000 rpm and 2500 rpm respectively. For an externally coupled generator, the nominal operating speed (ω_c) would be in the region of 6000 rpm. However, for an embedded S/G, which rotates with the engine shaft, the nominal speed would be in the range 15,000 to 20,000 rpm [9].

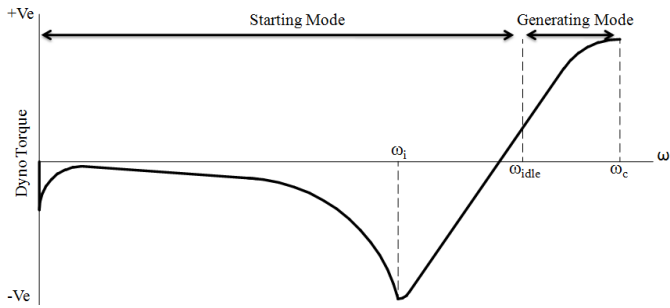


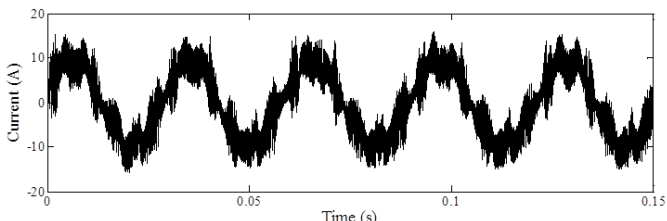
Fig. 7. Dynamometer torque-speed profile

VI. EXPERIMENTAL RESULTS

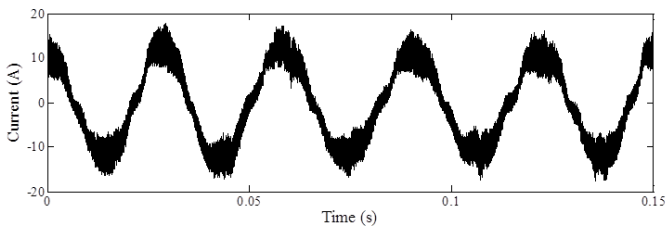
Results for each mode of operation are presented separately. In each mode conventional FOC and the PCC are subjected to the same testing conditions.

A. Starting Mode

In starting mode the power converter drove the S/G whilst it was mechanically loaded by the dynamometer. Waveforms are provided in Figure 8, which show a stator current of approximately 7 A_{rms} whilst the S/G rotated at 500 rpm. The upper plot shows the current when the converter was operating using conventional FOC, whilst the lower waveform is that achieved using the MBPCC.



(a)

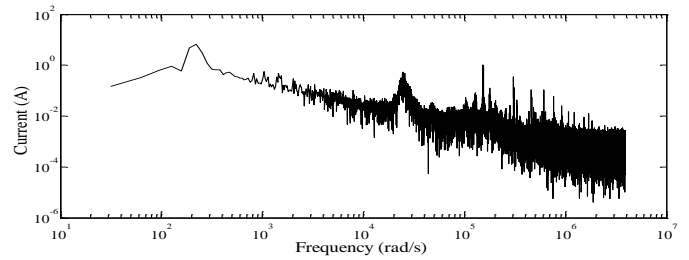


(b)

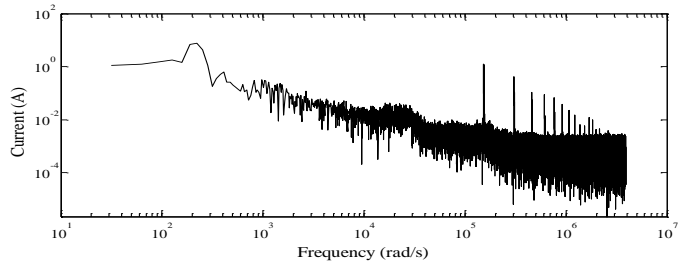
Fig. 8. Starting mode current waveforms (a) FOC control, (b) MBPCC

A power analyzer was used to examine the spectral content of the current. The spectra for the waveforms shown in Figure 8 are provided in Figure 9. The implementation of PCC provides a significant reduction in the THD of the stator current during starting mode. For the waveforms in Figure 8, the THD recorded by the spectrum analyzer was 40% and 17% for the conventional controller and MBPCC respectively.

The speed was varied between 100 and 700 rpm, whilst the power converter drove a stator current of 8 A_{rms} into the S/G. The results of this analysis, Figure 10, show a significant reduction in THD across the speed range using MBPCC.



(a)



(b)

Fig. 9. Starting mode current spectra (a) FOC control, (b) MBPCC

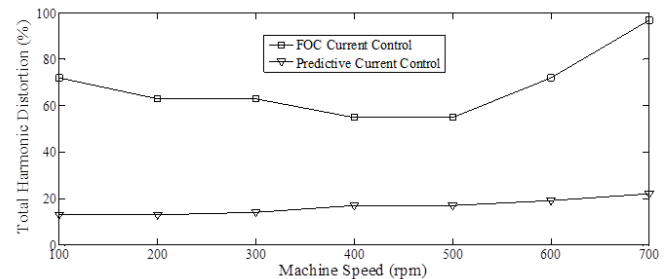


Fig. 10. Total harmonic distortion as a function of machine speed

B. Generating Mode

A similar study was undertaken to investigate the performance of the MBPCC with the system operating in generating mode. The dynamometer rotated the S/G at a constant 2500 rpm (ω_c), whilst the controller of Unit 1 was used to regulate the flow of electrical power into the utility network. Figure 11 shows the stator current waveforms obtained from one test where the feed in to the utility was adjusted to provide a stator current of 9.5 A_{rms}. The THD for these two waveforms was measured at 75% and 43% for the FOC and MBPCC respectively. The predictive controller is therefore providing a significant reduction of the THD during generation mode.

To further quantify the improvement offered by the MBPCC, the grid current was varied between 1 and 5 A, while the dynamometer maintained a constant speed of ω_c to assess the controller performance as a function of the real power delivered to the utility. The results provided in Figure 12 show MBPCC reduces the THD of the stator current. Also, the THD for both controllers improves as the utility current is increased which is to be expected since the fundamental component of the stator current increases with the power in order to maintain a constant DC link, while the majority of the other harmonics tend to remain at a constant amplitude.

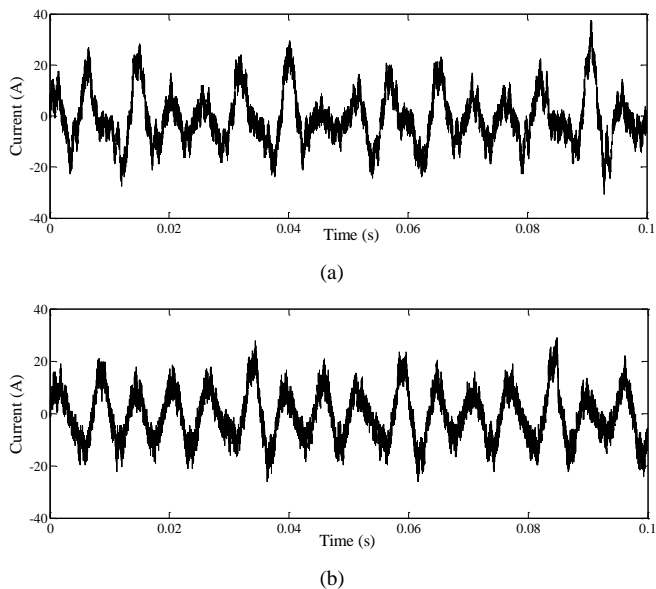


Fig. 11. Starting mode current waveforms (a) FOC control, (b) Predictive control

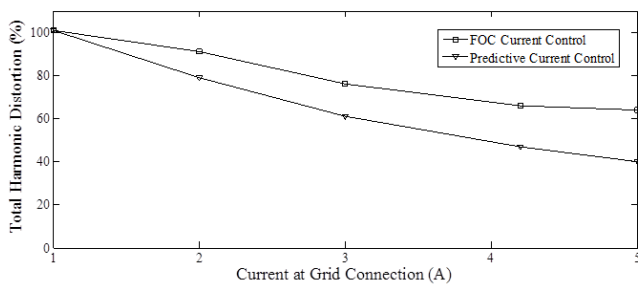


Fig. 12. Total harmonic distortion as a function of grid current

VII. CONCLUSION

This paper has described how model based predictive current control may be applied to a 5 level, diode clamped, multilevel converter based drive system for aerospace starter-generator applications. The combination of controller and converter topology ensures that the THD measured in the S/G's stator current waveform is reduced. MBPCC is compared to the industry standard FOC and is found to perform favourably, providing a significant reduction to the measured THD in both starting and generating modes, across a range of speeds and current levels.

REFERENCES

- [1] M. J. Provost, "The More Electric Aero-Engine: A General Overview from an Engine Manufacturer," at the Power Electronics Machines and Drives Conference, Bath, UK, 2002, pp. 246-251.
- [2] R. H. Williams, D. A. Stone, M. P. Foster, S. R. Minshull, "Back-to-Back Connected Multilevel Converters for Aerospace Starter-Generator Applications," Power Conversion Intelligent Motion Conference, Nuremberg, Germany, 2011, pp. 352-357.
- [3] R. H. Williams, D. A. Stone, M. P. Foster, S. R. Minshull, "Utilizing Existing Aircraft Wound Field Generators for Starter-Generators," in Proc. 8th International Conference on Power Electronics, Jeju, South Korea, 2011, pp. 691-696.
- [4] Department of Defence Interface Standard: Aircraft Electrical Power Characteristics, MIL-STD-704E, 1991.

- [5] SAE Minimum Performance Standards for Aerospace Electrical Power Converters, SAE-AS4361, 1991.
- [6] L. Andrade, C. Tenning, "Design of the Boeing 777 Electric System," NAECON, Dayton, Ohio, USA, 1992, pp. 1281-1290.
- [7] C. R. Avery, S. G. Burrow, P. H. Mellor, "Electrical Generation and Distribution for the More Electric Aircraft," Universities Power Engineering Conference, Brighton, UK, pp.1007-1012, 2007.
- [8] J. D. Ede, G. W. Jewell, K. Atallah, D. J. Powell, J. J. Allen, A. J. Mitcham, "Design of a 250kW, Fault-Tolerant PM Generator for the More-Electric Aircraft," Proc. American Institute of Aeronautics and Astronautics 3rd International Energy Conversion Engineering Conference and Exhibit, San Francisco, USA, 2005.
- [9] D. J. Powell, G. W. Jewell, J. D. Ede, D. Howe, "An Integrated Starter-Generator for a Large Civil Aero-Engine," Proc. American Institute of Aeronautics and Astronautics 3rd International Energy Conversion Engineering Conference and Exhibit, San Francisco, USA, 2005.
- [10] S.R. Minshull, C.M. Bingham, D.A. Stone, M.P. Foster, "A Back-to-Back Multilevel Converter for Driving Low Inductance Brushless AC Machines," at the European Power Electronics Conference, Aalborg, Denmark, 2007, pp. 1-9.
- [11] L.M. Tolbert, F.Z. Peng, T.G. Habetler, "Multilevel Converters for Large Electric Drives," IEEE Trans. of Industry Applications, Vol. 35, 2005, pp. 36-44.
- [12] D. Feng, B. Wu, S. Wei, D. Xu, "Space Vector Modulation for Neutral Point Clamped Multilevel Inverter With Even Order Harmonic Elimination," CCECE, Toronto, Canada, 2004, pp. 1471-1475.
- [13] S. R. Minshull, C. M. Bingham, D. A. Stone, M. P. Foster, "A New Switching Scheme for Reduced Switching Frequency and Balanced Capacitor Voltages for Back-to-Back Connected, Diode-Clamped Multilevel Converters," PEMD, York, England, 2008, pp. 65-74.
- [14] R. Kennel, A. Linder, "Predictive Control of Inverter Electrical Drives," Proc. IEEE Power Electronics Specialists Conference, Galway, Ireland, 2000, pp. 761-766.
- [15] J. Rodriguez, J. Pontt, C. Silva, "Predictive Current Control of a Voltage Source Inverter," IEEE Trans. Industrial Electronics, Vol. 54, pp. 495-503, February, 2007.
- [16] H. Moon, H. Kim, M. Youn, "A Discrete-Time Predictive Current Control for PMSM," IEEE Trans. Power Electronics, Vol. 18, pp. 464-472, January, 2003.
- [17] P. Wiparuramont, Z. Q. Zhu, D. Howe, "Predictive Current Control with Current-Error Correction for PM Brushless AC Drives," IEEE Trans. Industrial Applications, Vol. 42, pp. 1071-1079, August, 2006.
- [18] R. Vargas, P. Cortes, U. Ammann, "Predictive Control of a Three-Phase Neutral-Point-Clamped Inverter," IEEE Trans. Industrial Electronics, Vol. 54, pp. 2697-2704, October, 2007.
- [19] S. A. Verne, M. I. Valla, "Predictive Control of a Back to Back Motor Drive Based on Diode Clamped Multilevel Converters," Proc. 36th Annual Conference on IEEE Industrial Electronics Society, Glendale, AZ, USA, 2010, pp. 2972-2977.
- [20] E. H. J. Pallet, "Aircraft Electrical Systems," Longman, Third Edition.
- [21] I. Moir, A. Seabridge, "Aircraft Systems: Mechanical, Electrical and Avionics Subsystems Integration," Professional Engineering Publishing.
- [22] R. D. Flack, "Fundamentals of Jet Propulsion with Applications," Cambridge Aerospace Series, 2005.
- [23] D. Feng, B. Wu, S. Wei, D. Xu, "Space Vector Modulation for Neutral Point Clamped Multilevel Inverter with Even Order Harmonic Elimination," Proc. Canadian Conference on Electrical and Computer Engineering, Toronto, Canada, 2004, pp. 1471-1475.
- [24] D. G. Holmes, T. A. Lipo, "Pulse Width Modulation for Power Converters," Wiley-Interscience, 2003.
- [25] Texas Instruments Europe, "Field Oriented Control of 3-Phase AC-Motors," Available: <http://www.ti.com/lit/an/bpra073/bpra073.pdf>.
- [26] J. Pou, "Modulation and Control of Three-Phase PWM Multilevel Converters," Ph.D. dissertation, Dept. D'Enginyeria Electronica, Universitat Politecnica De Catalunya, 2002.
- [27] J. lai, F. Z. Peng, "Multilevel Converters - A New Breed of Power Converters," IEEE Trans. Industrial Applications, Vol. 32, June, 1996.